

# Chapter 11

## Industrial Robot–Integrated Fused Deposition Modelling for the 3D Printing Process

**T. S. Senthil**

*Panimalar Engineering College, India*

**R. Ohmsakthi vel**

*Chennai Institute of Technology, India*

**M. Puviyarasan**

*Panimalar Engineering College, India*

**S. Ramesh Babu**

*Sri Venkateswara College of Engineering, India*

**Raviteja Surakasi**

 <https://orcid.org/0000-0002-0786-0105>

*Lendi institute of Engineering and Technology, India*

**B. Sampath**

 <https://orcid.org/0000-0002-2065-6539>

*Muthayammal Engineering College, India*

### ABSTRACT

*In this chapter, six axis robots-integrated fused deposition modelling (FDM) processes have been used to fabricate the polymer three-dimensional (3D) printing objects. A unique method of printing 3D things uses an industrial robot with an FDM extruder as its end-effector. This robot is controlled by sophisticated controller technology and Robot Ware control software. The robot's end effector will travel along the designed toolpath as it is modelled by Robot Studio software. Printing a cube serves as a demonstration of the methods used to combine the FDM process with a six-axis industrial robot. This demonstrates how components can be produced using additive manufacturing and robotics. By applying different process parameters of the innovative system, the tensile and flexural strengths of printed specimens have been optimised using the Taguchi method.*

DOI: 10.4018/978-1-6684-6009-2.ch011

## **INTRODUCTION**

A three-dimensional object is created using the additive manufacturing technique of fused deposition modelling (FDM), in which material is deposited in horizontal layers on top of one another. A huge spool of thermoplastic material is used to feed a moving, heated extruder head with filament. An industrial robot is a mechanical device that can be programmed to undertake repetitive or risky activities with high levels of accuracy in place of a human. The welding, painting, assembly, pick-and-place work, packaging, palletizing, product inspection, and testing are typical uses for these robots. Extruder orientation changes and printing on inclination planes are not possible with traditional FDM machines. An industrial robot with an extruder as its end effector can be used to get around this. The goal of the current effort is to investigate a novel industrial robot application to get over the constraints of traditional machines. The current work's goal is to create an FDM method that is coupled with an industrial robot to print 3D items. Additionally, this project seeks to print items on curved surfaces, numerous planes, and inclined planes. The six-axis industrial robot has a maximum payload capacity of 6 kg. The extruder in this work is moved using quick programming (meant for ABB robot) commands. The STL file created from the 3D model is utilised as the input file. Using a MATLAB tool, it is divided into layers based on layer thickness. The influence of various operating parameters such as raster angle, layer thickness, deposition speed and deposition angle on tensile strength and flexural strength is evaluated. By extruding the same build material from both nozzles of the extruder attached to an industrial robot, a new method has been created to reduce printing time. The findings showed that the tensile and flexural strength are considerably influenced by the deposition feed rate, scanline width, and raster angle parameters. Contrary to the traditional FDM technique, which slices items parallel to the horizontal plane, an industrial robot has been created that can slice objects in a variety of planes. The outcomes showed that with the aid of the robot, homogeneous material deposition was seen at the intersection of the planes. Using the methodology, a NACA0015 airfoil-shaped section of an aeroplane wing is printed. The wing is cut in a series of concentric curves, and each layer's curved surface is also printed along. By using the industrial robot to deposit material over nonplanar layers, the staircase effect is minimised.

## **OVERVIEW OF FDM PROCESS USING INDUSTRIAL ROBOT**

The suggested system improves the CNC procedure. The proposed system only yielded a small number of prototypes, but the outcomes showed that the requisite dimensional accuracy was attained. In this study, a trajectory generating algorithm that creates trajectories for various paint thicknesses has been constructed. In this study, the deviation angle of the spray cone is adjusted via patch formation. The created trajectory generation algorithms have demonstrated a reliable level of performance, according to the paint thickness verification method (G. Q. Jin et al., 2013). A brand-new toolpath planning method for robotic manipulator applications like spray painting that is based on the CAD model of the work part. By segmenting the part's surface into smaller sections or patches, the system creates efficient toolpaths automatically. According to experimental findings, the technology that has been designed is useful for robotic applications. Aims to use a novel hybrid toolpath generating method to increase accuracy and decrease building time for additive manufacturing operations. To shorten the building time, algorithms were created to produce the toolpath for each slice based on its geometry. Applying the suggested tool route generating technique to five biomedical models produced successful results (Keating & Oxman,

2013). Additive, subtractive, and formative processes are all included in the multi-functional fabricating process known as robotic manufacturing. A robotic arm is created to do jobs like 3D printing, carving, and milling operations in the suggested fabricating process. It suggested that the robotic arm fabrication platform offers to work effectively and in a broader workspace (Y. an Jin et al., 2014). A 5-axis machine tool has a spindle and an FDM extruder placed on the opposite side of the rotary axis. After being printed, the FDM items can be machined to improve their dimensional accuracy (Ding et al., 2014). To create direction parallel toolpaths for the FDM process, a new method has been created. In order to reduce acceleration or deceleration when moving the tool from one location to another, parametric curves are used. This technology was used to fabricate various parts, and the results showed that the requisite efficiency and precision were attained (Allen & Trask, 2015). Toolpath generation algorithm for wire and arc additive manufacturing. Reduced starting and stopping positions are a goal of the algorithm. The industrial robot was used to create two pieces, one using the current hybrid technique and the other using the created algorithm (Song et al., 2015). Direct Energy Deposition (DED) techniques have an overhang/undercut problem, and it has been suggested to use tool mechanisms with more than three axes. To generate overhang features, a complex slicing technique was suggested for the control of tool paths on a 5-axis base table. The authors created and applied an auto-partitioning approach to produce 3D layer data for the multi-axis tool path (Lee & Jee, 2015). RevoMaker, a novel 3D printing method, can create items using less build material and less support material for overhangs. This “RevoMaker” was used to print several prototypes, and the findings showed that there was less material waste and the printing time was shorter (B. Huang & Singamneni, 2015). The foundation of the system is the use of six linear actuators to control the mobility of the platform. The faults that are produced during the printing process are corrected using a laser and camera system. Results showed that multidirectional printing allows for the printing of items with fewer support structures and without the staircase effect. A problem with the FDM process and created a fix for it. According to the scientists, the cited flaw in the existing printing technique can be fixed by deposition of material in curved layers utilising a parallel robot. According to authors, the staircase effect will cause the component printed using this method to have weak strength and bonding along the z-axis. According to the findings, printing durations for components with better surface finishes were also significantly shorter than those for components made using the traditional FDM process(Gao et al., 2015).A slicing algorithm for robotic material deposition systems to print structures with overhangs in many directions. The created algorithm makes various cuts in the STL model of the object. It has been shown that the suggested approach provides a straightforward method for slicing objects with sharp edges. To create parts with superior mechanical qualities, a research team has proposed curved layer adaptive slicing (CLAS), a revolutionary slicing technique for the FDM process. The object is adaptively divided into flat and curved layers using the CLAS approach. It said that applying CLAS to a test part revealed that its mechanical behaviour is comparable to the part that is printed traditionally(Y. Huang et al., 2016). In addition to preserving fibre continuity, CLAS is good at capturing sharply variable surface profiles and other finer component characteristics. Thicker curved layers produce better mechanical qualities, as demonstrated by three-point bending tests on light curved objects built of curved layers of different thicknesses.

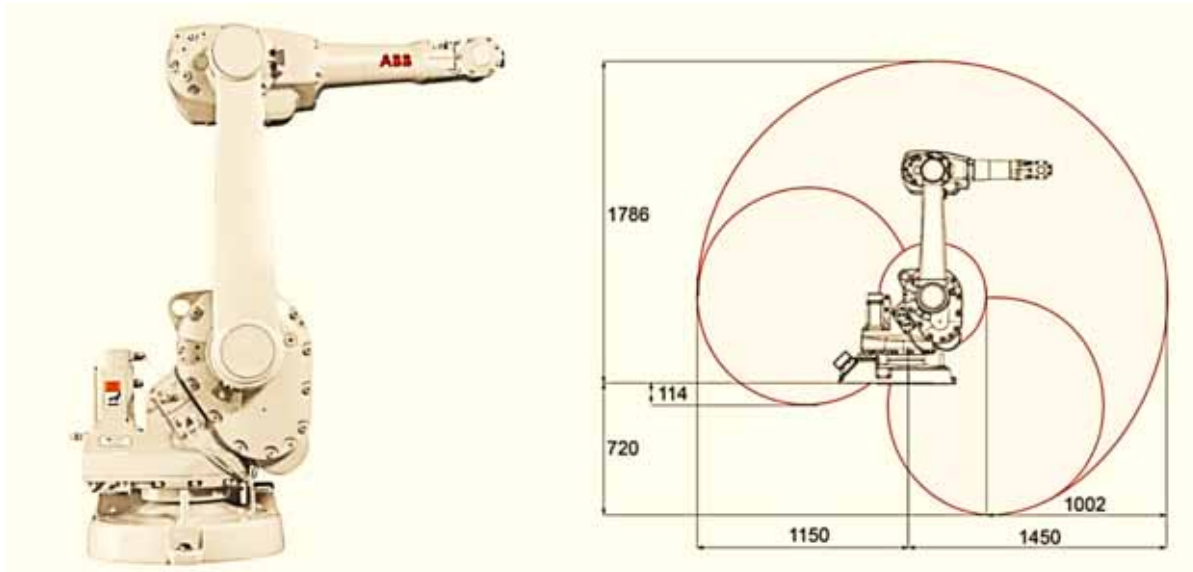
A robotic frame manufacturing algorithm that leads to a logical fabrication process. Based on the suggested methodology, a prototype was created and tested using a 6-axis robotic arm. It suggested that a variety of items that can be constructed using lightweight frames can be printed using the provided algorithm(Lim et al., 2016). Researchers have improved 3D printing using the spider's natural construction methods. Robot is programmed to print ABS-based 3D geometries in an open volume. The

findings showed that ABS material has insufficient strength and cannot be used for large-scale architectural printing(Yuan et al., 2016). Researchers at Aberystwyth University in the UK have created an AM fabrication device that uses a robotic arm to deposit the material in various planes. The staircase effect is eliminated by a 3D printer that can print parts in various planes, according to a study team at the University of British Columbia in Canada. According to the results, the suggested system may be used to print components with improved mechanical properties, and the surface quality of printed components has also improved(Y. Jin et al., 2017). A method of fabricating curved layers in concrete for large-scale building. Grasshopper script is used to build a zig-zag toolpath along the curved layers. A sizable three-axes, gantry-style printing device is used to carry out the printing(Ertay et al., 2018). To reduce retraction during printing, a novel route filling pattern for the FDM process has been created. In this approach, discontinuous deposition is also prevented. The entire region is divided into a number of smaller sub-regions and sub-paths in this work. A method has been created that uses a number of interconnected sub-paths to create a continuous path filling pattern. By avoiding retraction motions, the Fast Fouquémier Descent Manufacturing (FDM) method becomes more effective(Li et al., 2018). Assisted support structures are not needed when using the incline layer printing (ILP) technique to print overhang features in 3D. In this method, the object's overhanging feature is cut at an angle to prevent the nozzle from interfering with the previously deposited layers. In contrast to the base of a standard gable, more material is deposited at the point where two planes with different orientations meet (gable roof). Controlling the deposition of many planar layers at the same location in a geometrical structure necessitates the use of a different tactic(Zhao et al., 2018). Utilising a 6DOF industrial robotic arm, a revolutionary hybrid technology. The robotic arm is equipped with various interchangeable heads that can do both subtractive and additive operations. A milling tool is used for subtractive operations and an FDM extruder for additive activities. For this hybrid system, which consists of a heat bed and fixture configuration, an integrated platform is created. Multiple directions can be printed by a robotic arm, cutting down on building time and expense. This hybrid process can provide high-quality items. To create high-quality sculptures, material is removed with the milling tool as it is deposited in layers by the FDM printer(Kubalak et al., 2018). A method for the FDM process that uses a six-axis industrial robot to deposit material on an item to enhance its mechanical qualities. It said that the object's interlayer bonding would be improved by this skin. In this work, two tensile test specimens were printed in accordance with ASTM D638 specifications. An innovative method of producing printed items using the conventional FDM procedure and a skinned surface has been put forth by a research team. The mechanical qualities of the skinned specimen are superior to those of the conventionally printed specimen, according to the findings of the tensile test. [(IEEE Robotics and Automation Society et al., 2019) A technique for the FDM process that synchronises the material's extrusion rate with the tangential speed and deposition temperature when the material is deposited along curved routes By carefully managing the current supplied to the extruder's heater, the temperature is kept at the desired consistent level. The tangential velocity is tuned in relation to the rate of material deposition while taking the machine jerk into account. After applying this technology to various pieces, it became clear that the printed parts' dimensional correctness was better than it was using the traditional FDM procedure(Jensen et al., 2019). A 3D printing method that employs multiple mobile robots to manufacture massive, single-piece constructions. Using Open RAVE software, careful planning is done in this effort to prevent mutual encounters. Concrete is delivered to the printing nozzles through a pump mechanism. A group of researchers has created a 3D printing device that they believe is capable of printing well on-site. The researchers claim that it is more scalable and time-effective than existing 3D concrete printing processes since it uses movable robotic

arms to carry out printing. To increase the dimensional precision of the FDM procedure, a team from the University of Bristol created a robotic arm that can cooperate with a unique FDM extrusion head. In this work, a dedicated computer is regarded as the controller. Throughout the printing process, 1900 is used to regulate the extrusion temperature. According to the findings, the weight of the extruder setup and the robot's acceleration or deacceleration both have an impact on the printed part's dimensional correctness (Ishak & Larochelle, 2019).

An integrated method for multi-plane printing and 3D printing of lattice structures has been created by a research team. A 6-DOF robot arm platform for FDM and an interface programme to control the robot arm make up the system. The Microsoft Foundation Class (MFC) library was used in its development. Additionally, a simulation tool is created in MatLab to enable visual verification of the printing process. The 3D lattice structure with an overhang design is printed without the support structure using this integrated system. (Jiang et al., 2019). According to a study, print path and orientation have a significant impact on how much support material is consumed with printed goods. It implies that a fresh approach to support creation could save waste by as much as 50%. Applying the suggested technique could also cut down on production time and energy usage. According to the team's findings, printing parts required less material, time, and energy than traditional printing. To print 3D objects, there are two novel deposition techniques. The first is an additive manufacturing strategy based on extrusion with five degrees of freedom. In contrast to standard extruder-based additive manufacturing procedures, rounder surfaces are printed in this work with an improved surface polish. Researchers at the Massachusetts Institute of Technology have created a 3D printer that can produce complicated pieces devoid of support structures (MIT). It creates components for 3D printing by using a fixed extruder and an articulated robot arm with a build plate as the end effector. (Bhatt et al., 2020). For the FDM process, a novel slicing algorithm is used to reduce the staircase effect and print stronger objects. This technique is able to identify an object's curved surfaces and produce nonplanar layers for each of those surfaces. The programme produces toolpaths for the extruder that are free of collisions along the planar levels. On a 3DOF FDM machine,

*Figure 1. The Robot model and their working ranges*



a method for printing curved objects has been devised. The outcomes showed that, contrary to other reports, the printed objects exhibited a smooth surface finish due to the material being deposited along nonplanar layers. For the robotic printer, the researchers employed an algorithm to produce a toolpath with numerous directions. It has been asserted that the tensile strength of the specimens printed utilising the created technique is comparable to that of human hands. Tensile strength and young's modulus have been proven in tests to increase with increasing printing angle and decrease with decreasing layer thickness. In this study, a slicing method is designed to print thin shell objects with a robotic extrusion system and reorienting deposition platform. The goal is to manufacture items with overhanging features without the usage of support structures at 3D printer speeds up to 10 times faster than conventional techniques. Because there is no need to print additional material for the support framework, the build time is dramatically reduced. It claimed that because the suggested technology can print nonplanar layers, the surface smoothness is also improved.

## **INDUSTRIAL ROBOT INTEGRATION FOR FUSED DEPOSITION MODELING PROCESS**

An industrial robot with an FDM extruder as its end-effector is used in a novel approach to print 3D things. In additive manufacturing, it is ideal to combine the fused deposition modelling technique with a 6-axis industrial robotic arm. This chapter describes several elements that went into this integration. Short cycle times and good path accuracy are characteristics of this robot. Arc welding, grinding, material handling, and deburring applications are better suited for it. Industrial robot ABB IRB 1600 has 6 DOF, a 6 kg payload capacity, and a 1.45 m reach. The robot has a position repeatability of less than 0.05mm. The six-axis robot model and their working ranges are illustrated in Figure 1. The motion ranges and motion speeds of six axis robot are shown in Table1.

Each of the robot's six joints is moved by powerful servo motors. These joints all revolve around a common axis. There are two groups assigned to these axes. Because they are used to place the wrist at the proper area in the workspace, the first three axes are known as the main axes.

*Table 1. Motion ranges and motion speeds of six axis robot*

Joint	1	2	3	4	5	6
Range (°)	±180	+150 to - 90	+65 to – 245	±200	±115	±400
Speed (°/s)	180	160	170	320	400	460

The fifth-generation Industrial Robot Controller (IRC5) uses a system-level controller and a servo-loop controller to govern how the robot moves. Industrial robots frequently carry out machining tasks like cutting and stamping. Robot controller technology is standardised by the IRC5, according to the robotics industry. It offers support for PC tooling, flexibility, safety, modularity, application interfaces, and multi-robot control. It has been discovered that the servo controller is the primary bottleneck con-

trolling the accuracy of the robot operations. A robot is an autonomous machine with three primary components that all function cohesively. The controller, actuator, and sensors make up the three essential components. Robot control systems regulate and direct the robot's operations to produce the intended outcome. The robot's movements is managed by the fifth-generation Industrial Robot Controller (IRC5). All the programmes required to control the robotic arm are included in here, which is the system's main brain. Controlling four drive modules that can drive 36 axes is made easier by the IRC5 controller.

The user interface between the operator and the controller is the Flex Pendant, also known as the Teach Pendant. It has both hardware and software and performs a variety of tasks to control the robot. The Flex Pendant has a joystick that may be used to jog the robotic arm and direct its movements.

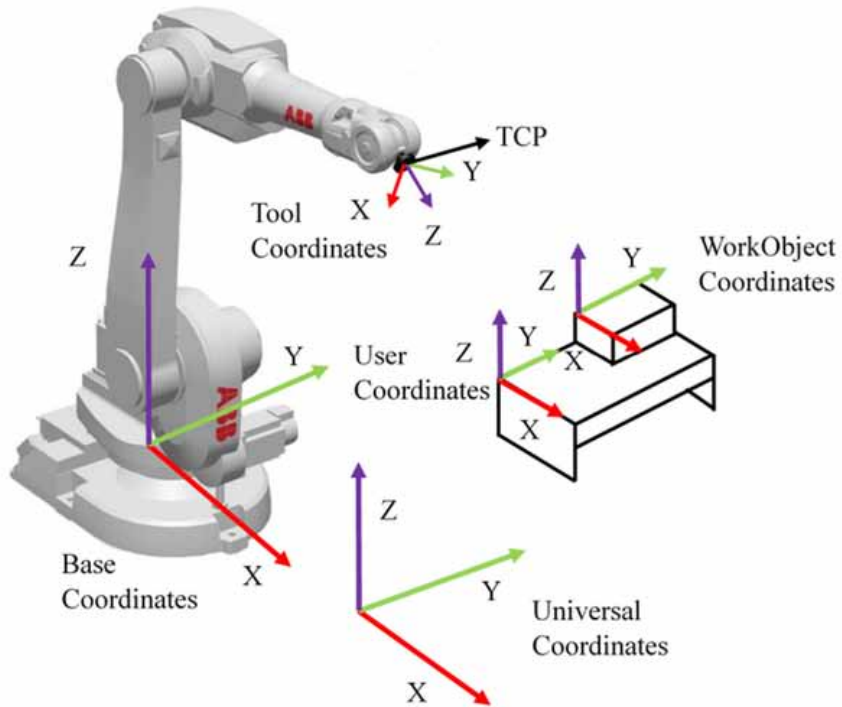
## **Robot Coordinate System**

At the apex of the hierarchy, a universal or world coordinate system stands in for the entire robotic work cell. In light of this, other coordinate systems, such as base coordinate, tool coordinate, work object coordinates, and user coordinate systems, are created. In the robotic work cell, each robot has its own base coordinate system. The various coordinate system of the robot is shown in Figure 2. Tool Center Point is the coordinate system's intersection point for all axes (TCP). When performing the task as specified by the operator, the robot moves the TCP along the predetermined spot. When work object coordinate systems are established with reference to the position of the work object, it is possible to easily alter the robot programmes with an offset if the workpiece's location changes. To make the programming step easier, reference points are created using a user coordinate system.

## **Rapid Prototyping Programming**

Robots from ABB are programmed using the high-level programming language Rapid. This programming language's objective is to construct a sequential path that the robot can follow to complete the desired tasks. Each module in a robot programme has a set of routines. An instruction set makes up each routine. Target instructions, Motion instructions, and Digital Output instructions were all employed in this project. These commands specify how the robot's end-effector is to move to the desired location. End effectors are the sections of the robot that communicate with other elements or objects in the surrounding space. A robot's arm's end effectors, which are used to move and position items, are located there. These robots will be capable of picking up, carrying, and setting down objects. Robot movement can be divided into three categories: circular, joint, and linear. Servo robots are equipped with manipulators, effectors, and robotic appendages that serve as the robot's hands and arms. The components of the robot that carry out the work are called effectors. Any tool that you can mount on your robot and operate with its computer is an effector. They are frequently tailored to the jobs that you want your robot to perform. The most widely used AM technology at the moment is FDM. High-strength thermoplastic components can be manufactured using this technique. The component of the 3D printer that propels the filament, melts it, and deposits it on the bed to construct the model is called an extruder. It is utilised for a variety of hues. mechanically robust and long-lasting. Removal is supported by hands-free. most Stratasys FDM 3D printers are compatible with it. Excellent ratios of cost to quality and cost to performance.

*Figure 2. Various Coordinate system of the Robot*



## **Robot Studio Software**

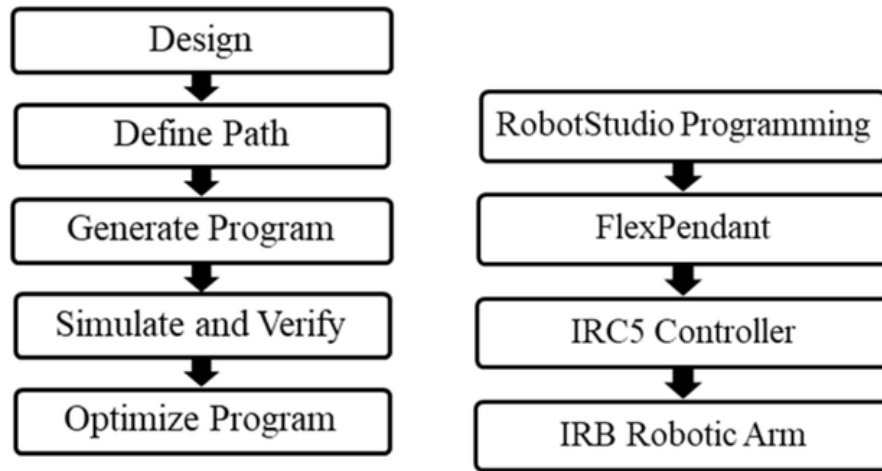
Robot Studio is a simulation programme used to visualise and programme the ABB robots in offline mode on a computer. Both actual and virtual robots can be managed using this. This simulation environment can be used to construct virtual robots and tools. Within this environment, work objects and TCPs (Tool Center Points) can be created.

With this software, CAD models may be imported as well as designed. Based on the CAD data, the software enables the programmer to construct precise placements. Utilizing the “play” and “synchronise” options will replicate the journey. The programme will generate errors if there are any singularity or reachability problems. By highlighting problems in the early phases of a robot’s development, simulation software is tremendously helpful in reducing the programming time. These mistakes can be fixed by altering the course. The generated software can also be altered. To perform the appropriate duties, this application can be uploaded to the actual robotic cell.

## **Instruction for Robot Motion Control**

The programme is originally built using the simulation application Robot Studio. After that, a USB drive is used to upload it to the flexible Pendant. The drive module will provide electricity to the robotic arm’s joints. They will be turned at a particular angle in accordance with the controller’s instructions. The robot arm’s movement is managed in this manner. The procedure and instructions used in the Robot Studio software are displayed in Figure 3.

*Figure 3. Procedure and Instructions for Robot Studio software*

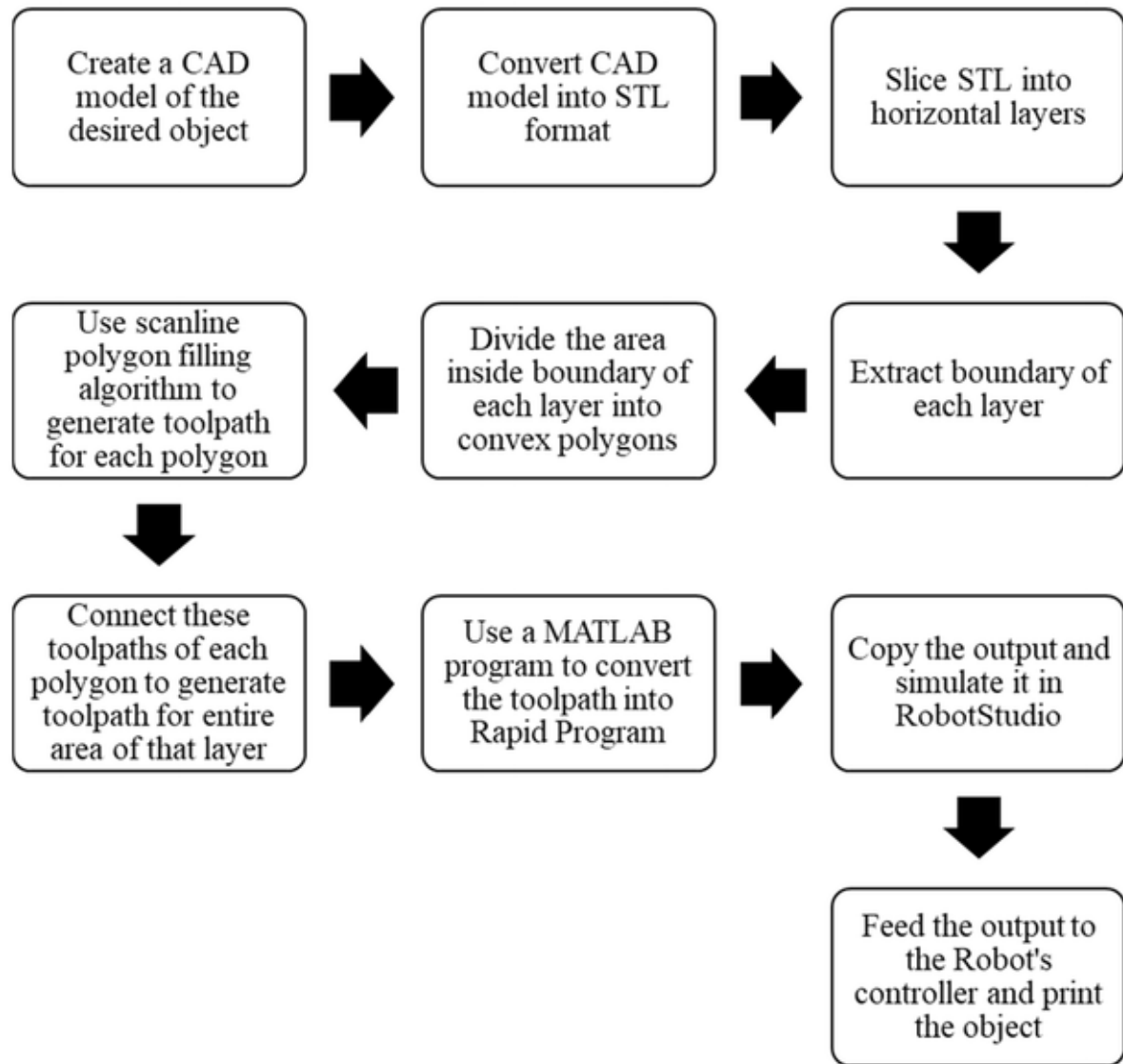


## METHODOLOGY FOR INTEGRATING INDUSTRIAL ROBOT WITH FDM EXTRUDER

This section outlines the process used to print an object with an industrial robot. The sequential processes for robot integrated 3D printing is illustrated in Figure 4.

- Making a CAD model of the object is the initial stage in this process. Making it with design software like CATIA is one method to do it. The alternative method involves creating a CAD model of an existing part using a 3D scanner.
- The process of converting a 3D model of an object into the format required for 3D printing comes next. In the STL format, triangles are used to roughly represent the object's surface rather than squares and rectangles as in the preceding example.
- The next step is to slice the CAD model using a horizontal plane after it has been converted into STL format. Up until the entire object is sliced, this plane's vertical increment is used. Each layer's thickness is then considered to be equivalent to the layer thickness in this example.
- This stage involves extracting a set of boundaries that are spaced apart by the same amount as the layer thickness. The following step is extracting each layer's border. If the boundary is a convex polygon, no additional processing is necessary to construct the toolpath.
- A line segment can be used to separate a concave polygon into convex polygons. Some of the diagonals of a convex polygon are outside the polygon. It features at least one interior angle that is close to 180 degrees.
- Based on the information gathered from the layer boundary, a toolpath is constructed. The same algorithm may be applied to concave and convex polygons as well as convex and concave boundaries. The required toolpath is generated by this algorithm using the input of the polygon's vertices.
- Using a customised MATLAB application, the technique is applied to produce the toolpath. The scanline polygon filling procedure is used for each of the individual convex polygons if the boundary is shaped like a concave polygon. The MATML application will be used to create a zigzag toolpath.

*Figure 4. Sequential processes for Robotic Printing*



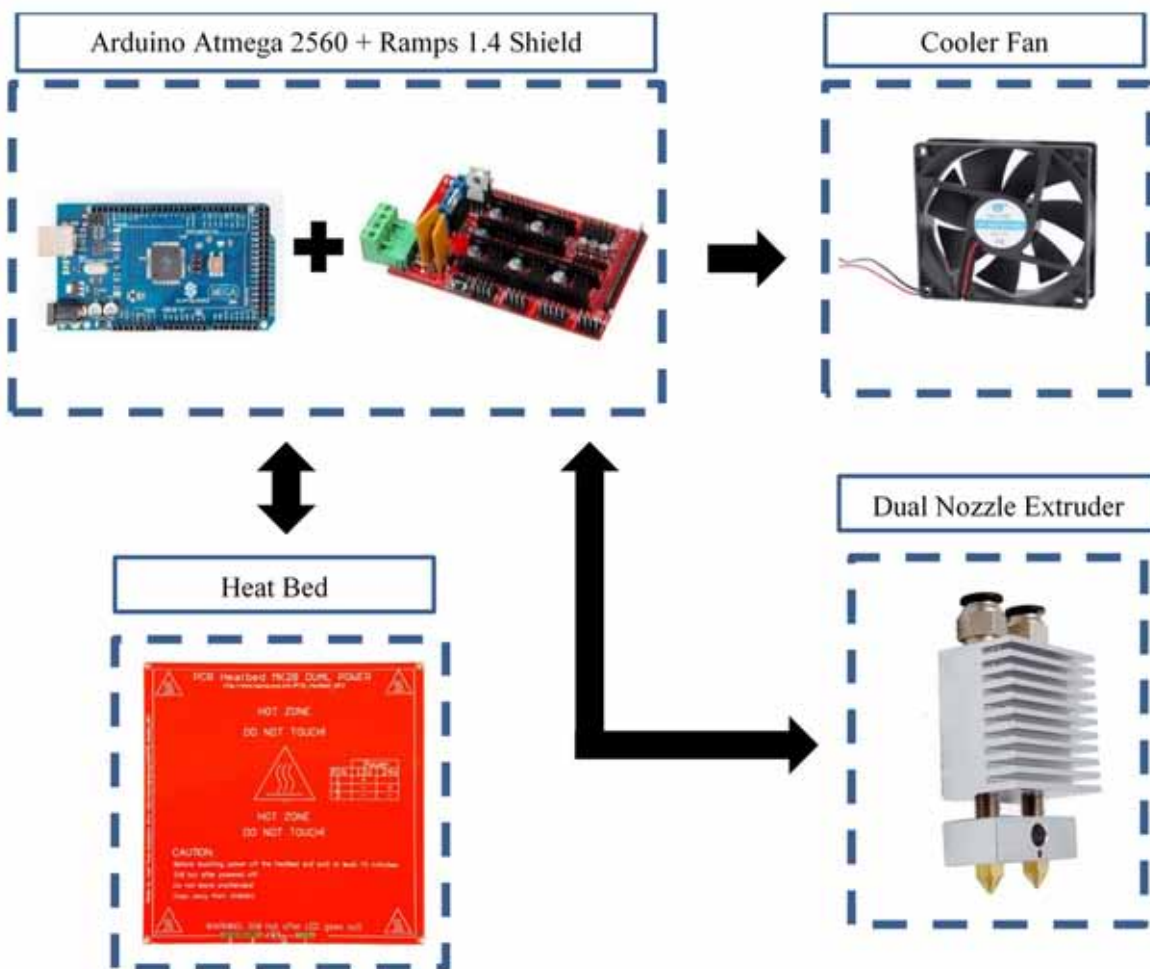
- Similar to levels on a 3D computer network, toolpaths are generated for each layer of an item. Using the extruder, the robot must deposit material at specific points along the toolpath. These segments are picked based on the sequence in which a computer sent the digital output signals to it.
- In a simulation environment, an ABB IRB 1600 robot is imported, and the flange of a two-nozzle extruder model is attached. TCP is simulated in a virtual environment that has been loaded with a quick software. The logs show any reachability or presence of singularity errors that may have occurred.

- A quick programme is performed, and then the robotic arm prints the desired thing. The programme is loaded into the actual controller after this simulation has been verified in the Robot Studio software.

## FDM EXTRUDER AND HEAT BED SETUP

This is the first time that PLA (polylactic acid or polylactide) material has been deposited by a robot in an industrial setting. A dual nozzle extruder was used to deposit the material in a controlled environment while heating it to 195°C to melt PLA. Stepper motors are used to feed PLA into the heat block as 1.75 mm-diameter filament. The substance melts and is then forced into the nozzle. Due to its thermoplastic nature, the material that is extruded from the nozzle solidifies instantaneously when it is exposed to the outside atmosphere. The robot's temperature is maintained at 195°C with an Arduino board and a Ramps

*Figure 5. Various components of FDM Extruder and Heater*



1.4 Shield with continuous feedback control. On a thin glass plate that is set in front of the robot, the desired object is allowed to construct itself. To regulate the cooling of the deposition of material, this plate is positioned on a heat bed. The same Arduino board control with constant feedback is used to keep the heat bed's temperature at 70°C. The likelihood of thermal stress buildup and warping in the printed object owing to abrupt cooling is reduced by the use of a heat bed. The components' temperatures (heat block and heat bed) are attained in less than 5 minutes after the Arduino board is powered up.

## **COMPONENTS AND SETUP FOR FDM PROCESS AND INDUSTRIAL ROBOT**

Prior to being executed by the robot's primary computer, programmes are uploaded to the FlexPendant. These instructions include both digital output signals and motion instructions. The main computer in the controller processes these commands and activates the robot's joints appropriately to move toward the intended targets in the intended direction. The various components of FDM extruder and heater are illustrated in Figure 5. The components and their connections for the Robot-3D printer setup is illustrated in Figure 6.

L293D Motor Driver are available on every Arduino Uno board. Each motor feeds filament-shaped material into the nozzle's heat block. The stepper motor keeps its position and material deposition ceases if the output signal is set to "LOW." The I/O board processes the digital output signals.

In this study, two distinct stepper motors in a PLA extruder are controlled by two digital output signals. Material is deposited through the nozzle when the stepper motor turns and the Arduino board's input signal is "HIGH." If it is set to "LOW," the motor maintains its position and no material is deposited.

An exclusive module for the Arduino UNO Board is the L293D. A full-featured Arduino shield that can operate DC motors, stepper motors, and servo motors is included in this motor driver shield. Material is fed via the extruder's nozzles by each stepper motor.

The stepper motor's four-terminal wires are linked to the L293D motor shield's corresponding pins. The stepper motor will be powered on by the L293D motor shield if the digital input signal for the Arduino board is "HIGH." In this work, stepper motors of the Nema17 type are utilised. They have a 12V DC rated voltage. These motors have a holding torque of 0.52 Nm (Figure 7).

A glass plate's surface serves as the definition of a work object. The material is deposited between the desired targets while the first nozzle's tip (TCP) travels along the predetermined path. This relies on the digital signals the controller sends, as well as how near the cooler fan the nozzle is. The real time robot setup for 3D printing of models are photographed in Figure 8.

Figure 6. Components and their connections for the Robot-3D printer setup

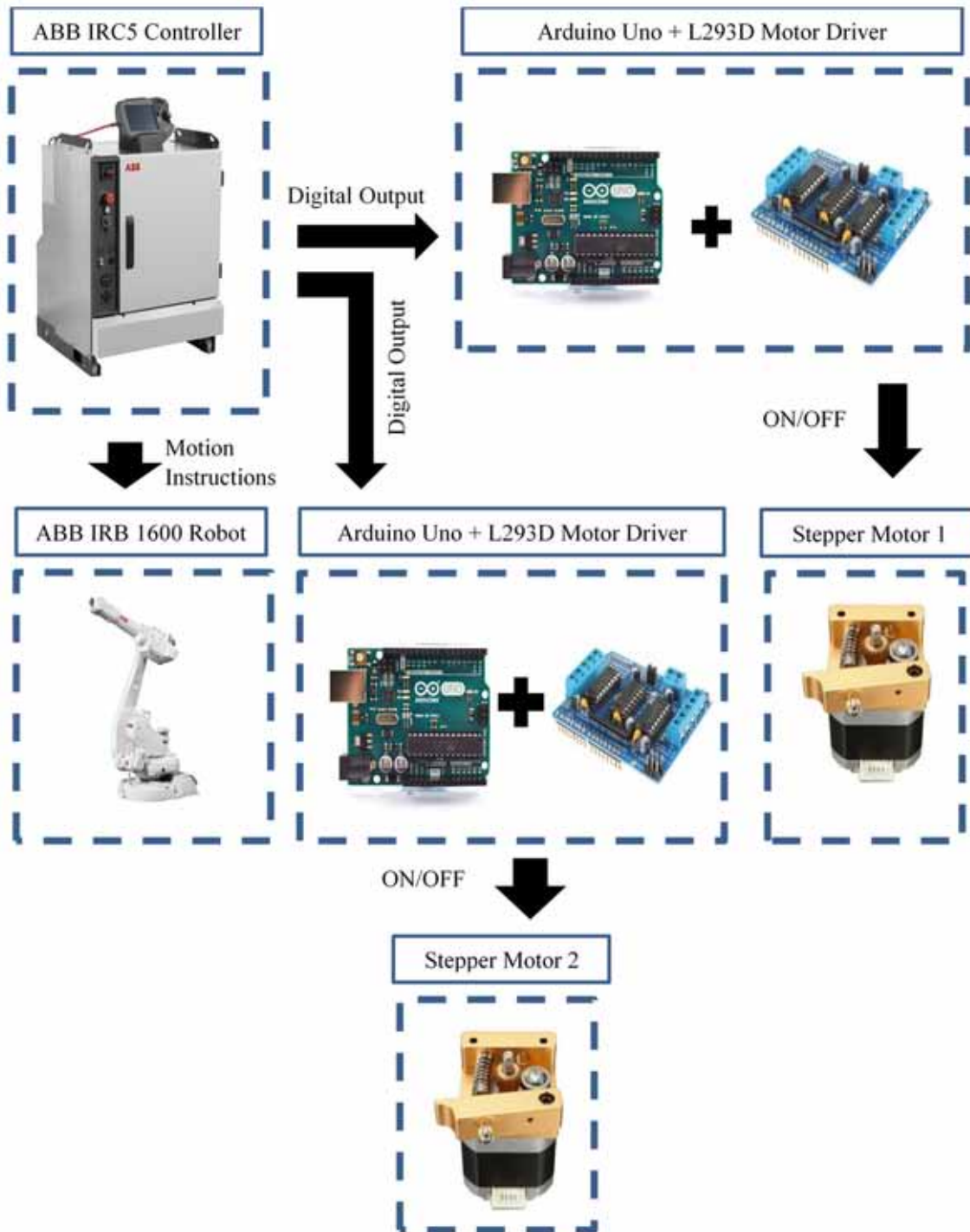


*Figure 7. Stepper motor controller*

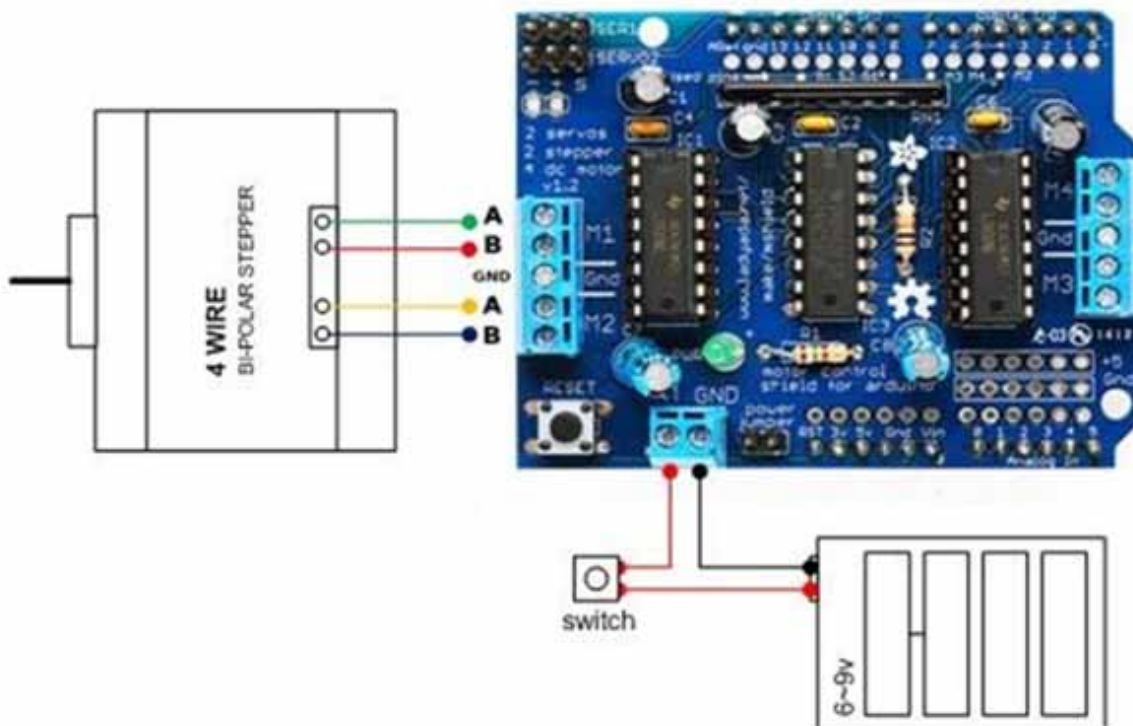


*Figure 8. Robot for 3D Printing Process*

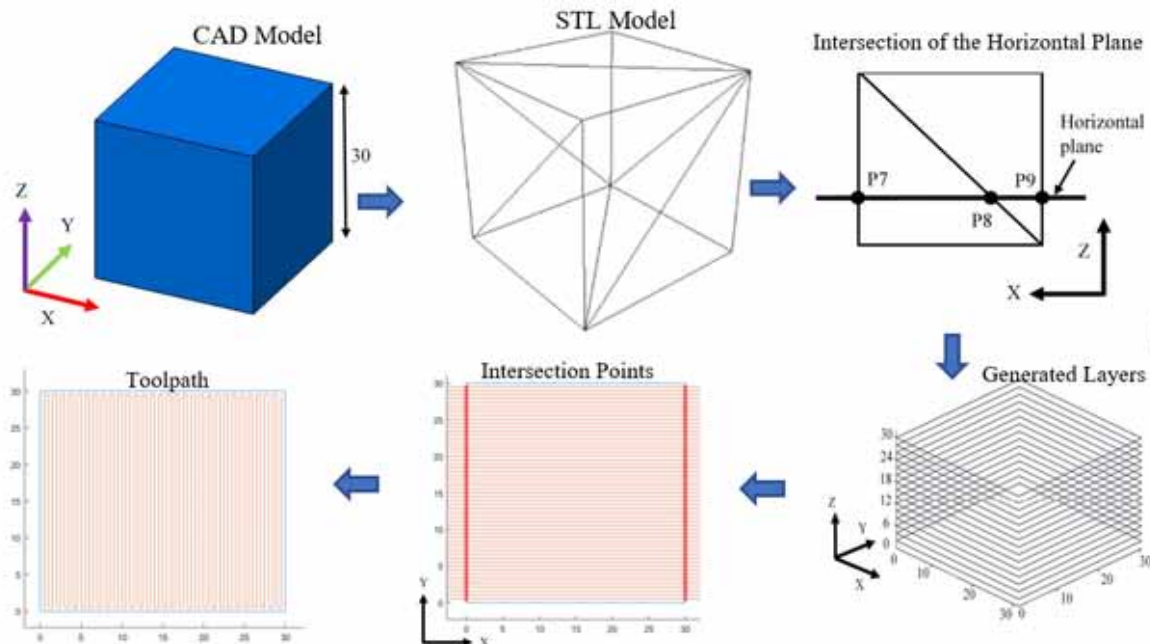


## PROCEDURE FOR INTEGRATING FUSED DEPOSITION MODELING PROCESS AND INDUSTRIAL ROBOT

How to simulate and print a cube using an industrial robot and FDM technology. The MATLAB programme is used to create a toolpath for material deposition, and it is translated into commands for the robot. Stepper motors are controlled to deposit material along the required route by using digital output signals. ABB Robot Studio simulation software is used to validate the generated toolpath. The influence of various operating parameters on the mechanical properties of the printed object is also presented in this chapter. The actual printing of the test part is done using the industrial robot after validating the generated toypath.

The methodology developed for printing 3D objects using the Industrial robot integrated with the FDM process is discussed in the previous chapter. The developed methodology was evaluated by printing a cube having an edge of length 30 mm. A horizontal plane that is parallel to the XY-plane is considered to slice the STL format of the cube to generate layers. The layer thickness considered to print the cube is 0.5 mm. This plane is incremented in the multiples of 1.5 vertically starting from the height of 0 mm till 30 mm. The horizontal plane is intersecting the cube at a height of 10 mm from the base, and it intersects the four faces of the cube. For each intersection, a set of intersection points are obtained. The horizontal plane is used to slice the cube along with the height in steps of 0.5 mm. After obtaining the intersection points, by joining all boundary points, the boundary of the layer at 10mm height is obtained. The different steps of FDM using industrial robot programming is illustrated in Figure 9.

*Figure 9. Fusion Deposition Modelling using Industrial Robot*

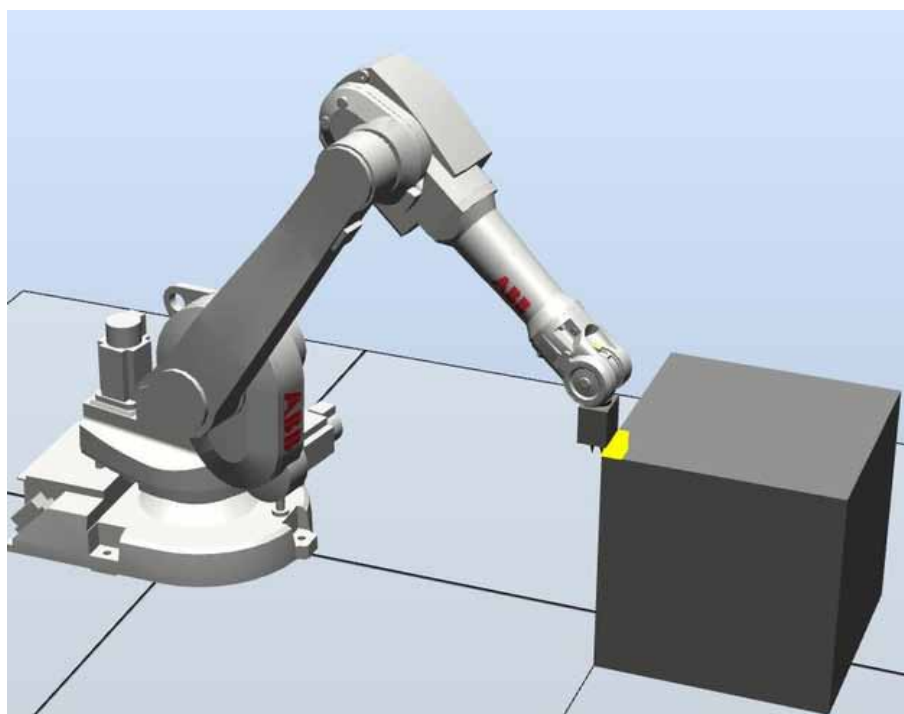


## **Generation of Toolpath**

The layers are laid out in a bottom-to-top approach, with the bottom-most layer selected to generate the toolpath. As the boundary of each layer is in a convex shape (square), the scanline polygon filling algorithm is directly applied. A scanline is used to intersect the sides of the square from bottom to top (towards positive Y-axis) with an increment of 0.5 mm to obtain a set of intersection points. This is done by a program that is developed in MATLAB software.

The direction of the infill's toolpath is set to perpendicular for any two consecutive layers. In this way, all the layers are scanned and a set of intersection points is obtained for each layer. A MATLAB program is used to generate the toolpath for the base layer of a digital image. As the considered boundary of the layer is in a convex shape, every horizontal scanline will intersect the sides of the square at two points i.e. left interaction point and right intersection point. Let's consider the left and right intersection points on a 2x2 grid. The left intersection point is H1 ( $H1X, H1Y, 0$ ) and the right intersection point as H2 ( $H2X, H2Y$ ). The coordinates of H2 are modified to ( $H2X-0.5, H2Y, 0.5$ ) using the same MATLAB program used to generate the toolpath for infill. The newly obtained set of modified intersection points are connected in a zig-zag fashion using the Jig-Jag program. For the next consecutive top layer (2nd) the direction of the toolpath for infill is perpendicular to the previous one. As it is scanned from left to right (towards positive X-axis), it intersects the sides of the square at two points i.e. bottom intersection point and top intersection point. The "y" coordinate of the bottom intersection point is subtracted by 0.5 mm from the top intersection point. This means that there is a gap between the toolpath on the top side and the infill on the bottom side. All the "y" coordinates of V2 are modified to ( $V2X, V2Y-0.5, 0.5$ ) and all

*Figure 10. Simulation of the robot integrated 3D Printing Process*



the intersection points are modified for the 2nd layer. This gives a gap between the toolpath of the shell and the infill on the top side. Toolpaths for all the even-numbered layers in the cube are generated in this way. The infill's direction of each layer is perpendicular to the direction of the next consecutive layer.

## **Simulation of the Printing Process**

The simulation of the robot integrated 3D Printing Process is illustrated in Figure 10. toolpath is generated by a command-line program that makes the extruder move linearly between two points at a velocity of 50 mm/s. The commands are then converted into digital output signals using the MATLAB program. All the motion commands are in form of MoveL statements that make the extrusion occur at a rate of 50mm/s or more. A rapid program is uploaded to RobotStudio software for validating the generated path. ABB IRB 1600 robot is imported into the simulation environment. Digital output signals are used to control the material deposition along the path. The velocity is considered based upon the viscosity of the PLA material and deposition feed rate just like a conventional FDM process. A dual nozzle extruder model is designed in CATIA software by considering the dimensions of the actual extruder. It has its nozzles separated by a distance of 20 mm, and is attached to the robot's flange via an international link-up system. A table model is created that resembles the printing bed. Workobject is defined on the surface of the table in such a way that the extruder model's orientation stays perpendicular to the table's surface. The virtual controller is created and the generated rapid program is uploaded to it.

## **Printing of Cube using the Industrial Robot**

The rapid code is uploaded to the IRC5 controller. After validating the simulation of TCP movement along the toolpath, the actual printing of the cube is carried out using the industrial robot. Objects with

*Figure 11. 3D Printed object*



overhanging structures can also be printed by depositing the support material where ever needed. An industrial robot has been developed which can be used as a material depositing machine for printing in the same way as a conventional FDM machine. The robot can print on inclined planes as well as on curved surfaces, according to researchers at the University of Bristol. The final product of the 3D printed object is shown in Figure 11.

## **TESTING OF MECHANICAL PROPERTIES OF 3D PRINTED PARTS**

The various process parameters to test the mechanical properties of 3D printed object is shown in Table 2. Engineering's understanding and analysis of any process or system's performance depend heavily on the experimental design, or planning of tests. The conventional method involves maintaining all the parameters constant while changing one parameter at a time. It takes a lot of time, necessitates running more experiments, and costs money. By using orthogonal arrays, Taguchi's resilient design gives each factor the same weight(Boopathi, 2021a; Boopathi et al., 2021b; Boopathi, Sureshkumar, et al., 2022; Myilsamy & Sampath, 2021; Sampath & Myilsamy, 2021). The chosen process parameters have a significant impact on the quality of the parts produced by the industrial robot. The mechanical characteristics of printed items are influenced by a number of process variables, including raster angle, layer thickness, deposition speed, and deposition angle.

*Table 2. Factors and their levels*

Factor	Raster angle (°)	Scanline width (mm)	Layer thickness (mm)	Deposition speed (mm/s)	Deposition feed rate (mm/min)	Deposition Angle (°)
Level	90-135	0.45, 0.5, 0.55	0.4, 0.5, 0.6	45, 50, 55	200, 220, 240	700, 900

The 6 DOF industrial robot that was employed in this project as the equipment for depositing the material provides the option to deposit the material at an angle. In order to examine its influence alongside the other components, this work has considered the deposition angle parameter. The angle at which a thin strip of thermoplastic material is extruded through the extruder's nozzle is known as the deposition angle. The thickness of the deposited layer is referred to as the layer's thickness. Layer width is referred to as raster width, while the space between two neighbouring roadways inside a layer is known as air-gap. To create an L18 mixed-level design with 6 components, the Taguchi method is utilised (Boopathi, 2022b, 2022a, 2022d, 2022c; Boopathi, Haribalaji, et al., 2022; Boopathi et al., 2023; Kannan et al., 2022; Kumar et al., 2023; Saravanan et al., 2022; Yupapin et al., 2022a). The extruder moves at a certain pace as it deposits material in the XY plane, which is known as the printing speed. Printing time is the total amount of time needed to print the object under consideration.

For tensile and flexural tests, specimens are printed in accordance with the L18 design matrix(Boopathi, Lewise, et al., 2022; Boopathi, Thillaivanan, et al., 2022; Gunasekaran et al., 2022; Sampath & N. Naveenkumar P. Sampathkumar, 2022; Trojovsky et al., 2023). These samples were examined using the Universal Testing Device INSTRON 3969. This machine was created specifically to perform tensile, compression, flexure, shear, and torsion testing. The procedure is inserting the test specimen into an

apparatus and exerting tension on it until it breaks. The gauge section's length is measured against the applied force as tension is applied. The industrial robot is used to print flexural specimens in accordance with ASTM D790 standard(Boopathi, 2021b; Boopathi et al., 2021a; Boopathi, Haribalaji, et al., 2022; Haribalaji et al., 2022; Jeyakymar et al., 2022; Kavitha et al., 2022; Yupapin et al., 2022b). The most used flexural test for thermoplastic specimens is the 3-point flexural bending test. The test specimen is put into the testing machine, and force is applied until the specimen breaks. Tensile specimen 11 achieves its maximum tensile strength. With a raster angle of 60°/150°, a scanline width of 0.45 mm, a layer thickness of 0.5 mm, a deposition speed of 45 mm/s, a deposition feed rate of 240 mm/min, and a deposition angle of 110°, this sample was produced. Deposition feed rate (which contributes 40.87 percent) has the greatest impact on tensile strength, while deposition speed has the least impact (0.94 percent). The deposition angle (36.79%) and scanline width (36.79%) have the greatest effects on flexural strength (1.24 percent).

## **SUMMARY**

An industrial robot with an FDM extruder as its end-effector is used in a novel approach to print 3D things. Robot Ware control software and a sophisticated IRC5 controller are used to control this robot. ABB Robot Studio software simulates how the robot's end effector will move along the created toolpath. Printing a cube serves as a demonstration of the methods used in this chapter to combine the FDM process with a 6-axis industrial robot. This shows that robotics and additive manufacturing can work together to produce components. On the tensile strength and flexural strength of printed specimens, the effects of different operation conditions are investigated.

## **REFERENCES**

- Allen, R. J. A., & Trask, R. S. (2015). An experimental demonstration of effective Curved Layer Fused Filament Fabrication utilising a parallel deposition robot. *Additive Manufacturing*, 8, 78–87. doi:10.1016/j.addma.2015.09.001
- Bhatt, P. M., Malhan, R. K., Rajendran, P., & Gupta, S. K. (2020). Building free-form thin shell parts using supportless extrusion-based additive manufacturing. *Additive Manufacturing*, 32, 101003. doi:10.1016/j.addma.2019.101003
- Boopathi, S. (2021a). An investigation on gas emission concentration and relative emission rate of the near-dry wire-cut electrical discharge machining process. *Environmental Science and Pollution Research International*, 29(57), 86237–86246. doi:10.100711356-021-17658-1 PMID:34837614
- Boopathi, S. (2021b). Improving of Green Sand-Mould Quality using Taguchi Technique. *Journal of Engineering Research*. doi:10.36909/jer.14079
- Boopathi, S. (2022a). An experimental investigation of Quench Polish Quench (QPQ) coating on AISI 4150 steel. *Engineering Research Express*, 4(4), 045009. doi:10.1088/2631-8695/ac9ddd

- Boopathi, S. (2022b). An Extensive Review on Sustainable Developments of Dry and Near-Dry Electrical Discharge Machining Processes. *Journal of Manufacturing Science and Engineering*, 144(5), 1–37. doi:10.1115/1.4052527
- Boopathi, S. (2022c). Cryogenically treated and untreated stainless steel grade 317 in sustainable wire electrical discharge machining process: A comparative study. *Environmental Science and Pollution Research International*, 1–10. doi:10.100711356-022-22843-x PMID:36057706
- Boopathi, S. (2022d). Performance Improvement of Eco-Friendly Near-Dry Wire-Cut Electrical Discharge Machining Process Using Coconut Oil-Mist Dielectric Fluid. *Journal of Advanced Manufacturing Systems*, 1–20. Advance online publication. doi:10.1142/S0219686723500178
- Boopathi, S., Balasubramani, V., Kumar, R. S., & Singh, G. R. (2021a). The influence of human hair on kenaf and Grewia fiber-based hybrid natural composite material: an experimental study. In *Functional Composites and Structures* (Vol. 3, Issue 4). doi:10.1088/2631-6331/ac3afc
- Boopathi, S., Balasubramani, V., Kumar, R. S., & Singh, G. R. (2021b). The influence of human hair on kenaf and Grewia fiber-based hybrid natural composite material: An experimental study. *Functional Composites and Structures*, 3(4), 045011. doi:10.1088/2631-6331/ac3afc
- Boopathi, S., Haribalaji, V., Mageswari, M., & Asif, M. M. (2022). Influences of Boron Carbide Particles on the Wear Rate and Tensile Strength of Aa2014 Surface Composite Fabricated By Friction-Stir Processing. *Materiali in Tehnologije*, 56(3), 263–270. doi:10.17222/mit.2022.409
- Boopathi, S., Lewise, K. A. S., Subbiah, R., & Sivaraman, G. (2022). Near-dry wire-cut electrical discharge machining process using water—air-mist dielectric fluid: An experimental study. *Elsevier: Materials Today: Proceedings*, 50(5), 1885–1890. doi:10.1016/j.matpr.2021.08.077
- Boopathi, S., Sureshkumar, M., Jeyakumar, M., Kumar, R. S., & Subbiah, R. (2022). Influences of Fabrication Parameters on Natural Fiber Reinforced Polymer Composite (NFRPC) Material: A Review. *Materials Science Forum*, 1075, 115–124. doi:10.4028/p-095f0t
- Boopathi, S., Thillaivanan, A., Pandian, M., Subbiah, R., & Shammugam, P. (2022). Friction stir processing of boron carbide reinforced aluminium surface (Al-B4C) composite: Mechanical characteristics analysis. *Materials Today: Proceedings*, 50(5), 2430–2435. doi:10.1016/j.matpr.2021.10.261
- Boopathi, S., Venkatesan, G., & Anton Savio Lewise, K. (2023). Mechanical Properties Analysis of Kenaf–Grewia–Hair Fiber-Reinforced Composite. In *Lecture Notes in Mechanical Engineering* (pp. 101–110). Springer. doi:10.1007/978-981-16-9057-0\_11
- Ding, D., Pan, Z., Cuiuri, D., & Li, H. (2014). A tool-path generation strategy for wire and arc additive manufacturing. *International Journal of Advanced Manufacturing Technology*, 73(1–4), 173–183. doi:10.100700170-014-5808-5
- Ertay, D. S., Yuen, A., & Altintas, Y. (2018). Synchronized material deposition rate control with path velocity on fused filament fabrication machines. *Additive Manufacturing*, 19, 205–213. doi:10.1016/j.addma.2017.05.011

- Gao, W., Zhang, Y., Nazzetta, D. C., Ramani, K., & Cipra, R. J. (2015). RevoMaker: Enabling multi-directional and functionally-embedded 3D printing using a rotational cuboidal platform. *UIST 2015 - Proceedings of the 28th Annual ACM Symposium on User Interface Software and Technology*, 437–446. doi:10.1145/2807442.2807476
- Gunasekaran, K., Boopathi, S., & Sureshkumar, M. (2022). Analysis of a Cryogenically Cooled Near-Dry Wedm Process Using Different Dielectrics. *Materiali in Tehnologije*, 56(2), 179–186. doi:10.17222/mit.2022.397
- Haribalaji, V., Venkatesan, G., Asif, M. M., Pandian, M., Subbiah, R., & Boopathi, S. (2022). Investigation on corrosion and tensile Characteristics: Friction stir welding of AA7075 and AA2014. *Materials Today: Proceedings*, 66, 743–748. doi:10.1016/j.matpr.2022.04.037
- Huang, B., & Singamneni, S. B. (2015). Curved layer adaptive slicing (CLAS) for fused deposition modelling. *Rapid Prototyping Journal*, 21(4), 354–367. doi:10.1108/RPJ-06-2013-0059
- Huang, Y., Zhang, J., Hu, X., Song, G., Liu, Z., Yu, L., & Liu, L. (2016). FrameFab: Robotic Fabrication of Frame Shapes. *ACM Trans. Graph. Article*, 3516(1112), 978–1. doi:10.1145/2980179.2982401
- Ishak, I., & Laroche, P. (2019). MotoMaker: A robot FDM platform for multi-plane and 3D lattice structure printing. *Mechanics Based Design of Structures and Machines*, 47(6), 703–720. doi:10.1080/15397734.2019.1615943
- Jensen, M. L., Mahshid, R., D'Angelo, G., Walther, J. U., Kiewning, M. K., Spangenberg, J., Hansen, H. N., & Pedersen, D. B. (2019). Toolpath strategies for 5DOF and 6DOF extrusion-based additive manufacturing. *Applied Sciences (Switzerland)*, 9(19), 4168. Advance online publication. doi:10.3390/app9194168
- Jeyakymar, M., Munusami, V., Shanmugam, P., Boopalan, N., Boopathi, S., & Sureshkumar, M. (2022). An investigation on wear loss and hardness of nitro-carburizing coated stainless-steel grade-316. *Materials Today: Proceedings*, 66, 1398–1404. doi:10.1016/j.matpr.2022.05.223
- Jiang, J., Xu, X., & Stringer, J. (2019). Optimization of process planning for reducing material waste in extrusion based additive manufacturing. *Robotics and Computer-integrated Manufacturing*, 59(January), 317–325. doi:10.1016/j.rcim.2019.05.007
- Jin, G. Q., Li, W. D., & Gao, L. (2013). An adaptive process planning approach of rapid prototyping and manufacturing. *Robotics and Computer-integrated Manufacturing*, 29(1), 23–38. doi:10.1016/j.rcim.2012.07.001
- Jin, Y., an, He, Y., & Fu, J. (2014). Optimization of tool-path generation for material extrusion-based additive manufacturing technology. *Additive Manufacturing*, 1, 32–47. doi:10.1016/j.addma.2014.08.004
- Jin, Y., He, Y., Fu, G., Zhang, A., & Du, J. (2017). A non-retraction path planning approach for extrusion-based additive manufacturing. *Robotics and Computer-Integrated Manufacturing*, 48(August), 132–144. doi:10.1016/j.rcim.2017.03.008

- Kannan, E., Trabelsi, Y., Boopathi, S., & Alagesan, S. (2022). Influences of cryogenically treated work material on near-dry wire-cut electrical discharge machining process. *Surface Topography: Metrology and Properties*, 10(1), 015027. Advance online publication. doi:10.1088/2051-672X/ac53e1
- Kavitha, C., Geetha Malini, P. S., Charan Kantumuchu, V., Manoj Kumar, N., Verma, A., & Boopathi, S. (2022). An experimental study on the hardness and wear rate of carbonitride coated stainless steel. *Materials Today: Proceedings*. Advance online publication. doi:10.1016/j.matpr.2022.09.524
- Keating, S., & Oxman, N. (2013). Compound fabrication: A multi-functional robotic platform for digital design and fabrication. *Robotics and Computer-integrated Manufacturing*, 29(6), 439–448. doi:10.1016/j.rcim.2013.05.001
- Kubalak, J. R., Wicks, A. L., & Williams, C. B. (2018). Using multi-axis material extrusion to improve mechanical properties through surface reinforcement. *Virtual and Physical Prototyping*, 13(1), 32–38. doi:10.1080/17452759.2017.1392686
- Kumar, P., Sampath, B., Kumar, S., Babu, B. H., & Ahalya, N. (2023). Hydroponics, Aeroponics, and Aquaponics Technologies in Modern Agricultural Cultivation. In Trends, Paradigms, and Advances in Mechatronics Engineering (pp. 223–241). IGI Global.
- Lee, K., & Jee, H. (2015). Slicing algorithms for multi-axis 3-D metal printing of overhangs. *Journal of Mechanical Science and Technology*, 29(12), 5139–5144. doi:10.1007/s12206-015-1113-y
- Li, L., Haghghi, A., & Yang, Y. (2018). A novel 6-axis hybrid additive-subtractive manufacturing process: Design and case studies. *Journal of Manufacturing Processes*, 33(March), 150–160. doi:10.1016/j.jmapro.2018.05.008
- Lim, S., Buswell, R. A., Valentine, P. J., Piker, D., Austin, S. A., & De Kestelier, X. (2016). Modelling curved-layered printing paths for fabricating large-scale construction components. *Additive Manufacturing*, 12, 216–230. doi:10.1016/j.addma.2016.06.004
- Myilsamy, S., & Sampath, B. (2021). Experimental comparison of near-dry and cryogenically cooled near-dry machining in wire-cut electrical discharge machining processes. *Surface Topography: Metrology and Properties*, 9(3), 035015. doi:10.1088/2051-672X/ac15e0
- IEEE Robotics and Automation Society, National Science Foundation (U.S.), & Institute of Electrical and Electronics Engineers. (2019). *2019 IEEE 15th International Conference on Automation Science and Engineering (CASE)*. Author.
- Sampath, B., Naveenkumar, P., & Sampathkumar, P. S. A. V. (2022). Experimental comparative study of banana fiber composite with glass fiber composite material using Taguchi method. *Elsevier: Materials Today: Proceedings*, 49(5), 1475–1480. doi:10.1016/j.matpr.2021.07.232
- Sampath, B., & Myilsamy, S. (2021). Experimental investigation of a cryogenically cooled oxygen-mist near-dry wire-cut electrical discharge machining process. *Strojniski Vestnik. Jixie Gongcheng Xuebao*, 67(6), 322–330. doi:10.5545/v-jme.2021.7161

Saravanan, M., Vasanth, M., Boopathi, S., Sureshkumar, M., & Haribalaji, V. (2022). Optimization of Quench Polish Quench (QPQ) Coating Process Using Taguchi Method. *Key Engineering Materials*, 935, 83–91. doi:10.4028/p-z569vy

Song, X., Pan, Y., & Chen, Y. (2015). Development of a low-cost parallel kinematic machine for multi-directional additive manufacturing. *Journal of Manufacturing Science and Engineering*, 137(2), 021005. Advance online publication. doi:10.1115/1.4028897

Trojovsky, P., Dhasarathan, V., & Boopathi, S. (2023). Experimental investigations on cryogenic friction-stir welding of similar ZE42 magnesium alloys. *Alexandria Engineering Journal*, 66, 1–14. doi:10.1016/j.aej.2022.12.007

Yuan, P. F., Meng, H., Yu, L., & Zhang, L. (2016). Robotic Fabrication in Architecture, Art and Design 2016. *Robotic Fabrication in Architecture, Art and Design*. Advance online publication. doi:10.1007/978-3-319-26378-6

Yupapin, P., Trabelsi, Y., Nattappan, A., & Boopathi, S. (2022a). Performance Improvement of Wire-Cut Electrical Discharge Machining Process Using Cryogenically Treated Super-Conductive State of Monel-K500 Alloy. *Iranian Journal of Science and Technology. Transaction of Mechanical Engineering*. Advance online publication. doi:10.100740997-022-00513-0

Yupapin, P., Trabelsi, Y., Nattappan, A., & Boopathi, S. (2022b). Performance Improvement of Wire-Cut Electrical Discharge Machining Process Using Cryogenically Treated Super-Conductive State of Monel-K500 Alloy. *Iranian Journal of Science and Technology - Transactions of Mechanical Engineering*, 1–17. doi:10.1007/s40997-022-00513-0

Zhao, H., He, Y., Fu, J., & Qiu, J. (2017, November). Inclined layer printing for fused deposition modeling without assisted supporting structure. *Robotics and Computer-integrated Manufacturing*, 51, 1–13. doi:10.1016/j.rcim.2017.11.011